

Highly sensitive magnetometers—a review

D. Robbes*

CNRS - Groupe de Recherche en Informatique, Image, Automatique et Instrumentation de Caen, 6 Boulevard Maréchal Juin,
F-14032 Caen Cedex, France

Received 23 September 2005
Available online 19 January 2006

Abstract

Conventional magnetic sensors, easy to use, are supposed to work mainly well over the nanotesla range, as due to the large magnetic environmental noise occurring in urban and industrial environments. On the other hand, a strange world exists, well below the nanotesla range, where the very efficient magnetic properties of superconducting materials have been used. It is the world investigated using cryogenic sensors, especially those of the SQUID's family. During a long time starting from the 1960s, SQUID people have refined their technologies, together with the use of advanced signal processing both analogue and digital, in order to input couple various external magnetic sources at room temperature, such the bio magnetic ones. State of the art of SQUID sensors is given. In the early 1990s, the dramatic improvement of the operating temperature led to the hope of lighter and lower costs systems with reduced cryogenic mount, designed to operate in open environment. An important target of multi SQUID systems using high critical temperature superconductors was and still is the magnetocardiography (MCG) mapping that could be daily used for improved diagnosis, as compared to conventional electrocardiography. It is known that such an important application is realistic only with noise spectral densities referred at the input lower than $100 \text{ fT}/\sqrt{\text{Hz}}$ in a frequency bandwidth lying in between 1 Hz and 1 kHz and with a spatial resolution lower than 1 cm. The talk will review the recent advances in room temperature solid state sensors that could reach the above specified noise level. The review includes: magnetoresistive devices (AMR, GMR, spin valve, and spin dependent tunnelling device), Giant magneto-inductive devices. Non-solid, atomic vapor laser magnetometers, which have recently shown their ability to deliver very clear MCG signals, and start to be used to map the MCG signal above the chest just like SQUIDs systems, are reviewed. A simple, convenient energy resolution—volume is proposed, which allows a convenient way to compare high sensitivity magnetic sensors.

© 2006 Elsevier B.V. All rights reserved.

Keywords: Magnetic field sensors; SQUID; GMR; Spin valve; Magnetic tunnel junction; Atomic vapor magnetometer

1. Introduction

This review on highly sensitive magnetometers is proposed in the spirit of a previous one [1], which was addressed to the community of researchers involved in applied superconductivity, especially superconductivity applied to electronics and sensors. By that time, during year 2000, more than 15 years after the discovery of high critical temperature (T_c) superconductivity [2] in perovskites, especially in the famous $\text{YBa}_2\text{Cu}_3\text{O}_{7-\delta}$ compound which was quickly synthesised as thin film on various substrates [3], people had fabricated many of the circuits designed earlier using low T_c superconductors. Although the fabrication of good quality Josephson junctions on large scale was found to be rather difficult, it was quickly shown that grain boundaries that occur at misoriented crystals [4] exhibited the necessary

Josephson effects, leading to easy, single layer technology (but small scale) with thin film deposited on bicrystals. Fabrication processes of the famous quantum interference devices, namely the SQUIDs, both in the dc and rf schemes were then possible. During the 1990s, many successful devices were made which show the intrinsic low noise properties of high T_c SQUIDs lying in the range of $10\text{--}50 \text{ fT}/\sqrt{\text{Hz}}$, even at frequencies as low as 1–10 Hz. These performances are known to be very well matched to some biomagnetism applications, especially magnetocardiography [5,6]. SQUID people then dreamt to large applications and market for high T_c SQUIDs systems operating at 77 K, or slightly less, using either easy liquid nitrogen cooling or various light cryocoolers. These systems were designed to operate in open environments, i.e. with the magnetic sources to be measured lying in standard noisy conditions, as encountered in urban hospital or industry buildings. Open environment also means an operating range large enough for the SQUID to support the earth magnetic field. Unfortunately, although robust systems

* Tel.: +33 2314526; fax: +33 2314526.

have been demonstrated, and in spite of efficient denoising processes, the full SQUID sensitivity was almost never used in these very hard conditions, where too many orders of magnitude of environmental noise are involved, leading to a (post processed) background noise level lying within $100 \text{ fT}/\sqrt{\text{Hz}}$ to $1 \text{ pT}/\sqrt{\text{Hz}}$ [6,7]! Noting this difficulty, together with some more or less subjective barrier to the necessary cryogenic operation in the head of companies' engineers, the end of the nineties turned to be rather pessimistic for a large development of high T_c SQUIDS systems. Finally the dream vanished, and many SQUIDS people returned to low T_c devices. Nevertheless, some of these researchers came to room temperature magnetic sensors, to have a look on high sensitivity magnetometers, with in mind that their large knowledge about magnetic noise and associated denoising techniques could help to achieve new devices and systems, hopefully operating from the $100 \text{ fT}/\sqrt{\text{Hz}}$ level above 1 Hz compatible with interesting, middle sensitivity, SQUIDS applications. Finally, with the 2004 EMSA Conference, I thought it was an appropriate time to update the review made earlier on high sensitivity magnetometers.

The paper is arranged as follows: Section 2 will summarize the most relevant parameters to be used when addressing the area of high sensitivity magnetic field sensors. Those people familiar with sensor specifications, especially for the noise, can leave out that section. Section 3 will give a compact idea of state of the art SQUIDS sensors, having in mind that SQUID systems and major applications cannot be presented here. Section 4 will introduce recent developments in atomic vapor magnetometers which have shown remarkable performances, down to the $\text{fT}/\sqrt{\text{Hz}}$, at room temperature. Section 5 briefly discusses some of room temperature solid state devices, such giant magneto-resistive based devices (GMR), and giant magneto-impedance devices (GMI), and more exotic ones.

2. Highly sensitive magnetometers: relevant parameters

Dealing with the subject of sensitive magnetometers needs some starting definitions and limitations because of an area which quickly can reveal very large. In my mind, the expression "relevant parameters of a sensor" means those parameters that are required by engineers to choose and buy sensors when designing operating systems for specified applications. In this way, researchers designing possible new sensors at best must give some specifications as listed below, which greatly exceeds specification of the only basic sensor sensitivity. Of course, even though the preliminary studies starts from that quantity, authors should quickly take care to other important specifications: noise equivalent field at the input, bandwidth and slew rate, dynamic range and linearity, energy and spatial resolutions, gradiometer association, cross-talk and network associations, compatibility with silicon integrated circuits, compatibility with digital signal processing, temperature effects, etc.

Let us introduce some notations relative to these sensor specifications. First is the sensitivity to one physical quantity (magnetic field component or magnitude), also known as the transfer

function from the input (magnetic field) to the output (voltage) S_B^V (V/T), which generally is frequency dependent. Note that the available performances of the sensor itself seldom are relevant. Practically, a biasing system and some preamplifier often are necessary to get the full performances. In the following, bias and preamp are included. Dealing with high sensitivity sensors allows to have typically high transfer coefficient, as high as 10^5 V/T , value compatible with operation in earth magnetic field where 10 V at the output correspond to $100 \mu\text{T}$. A quick, rough, thought process allows to sense in advance that the operating range of practical systems with such a transfer value can be very large. Using standard low noise electronics, we for example know that an operational amplifier may work over 10 orders of magnitude (say 1 nV to 10 V). Let us then straightforwardly divide $100 \mu\text{T}$ by 10^{10} to get 10 fT, which give a quick idea of how low the electronic limitations could be! Finally, in my mind, high (field) sensitivity also means sensors having a large or very large working range from fT up to μT .

The second important specification is the intrinsic noise of the sensor, conveniently referred at the sensor's input, in units of the square root of an equivalent magnetic power spectrum, $B_{n,\text{eq}}(f)$ where f is the frequency. Practically, the time variations of the output voltage are recorded, followed by a Fourier transform, and then divided by the transfer function $S_B^V(f)$ to get $B_{n,\text{eq}}(f)$, expressed in $\text{T}/\sqrt{\text{Hz}}$. Once this is properly done, the noise specification is truly useful only if the intrinsic noise of the sensor is the dominant one, otherwise it should be specified which source is probably dominating. This means that the noise is not directly given by the noise coming from the electronic (bias and/or preamp). The latter is usually easy to compute from the circuit and data sheets and easy to measure. This also means that the noise at the sensor's output is not some environmental noise, i.e. coming from external noise sources and finally properly measured by the sensor. To reduce such environmental noise needs to be very careful, with the use of sufficient magnetic shields, which cannot be improvised, especially at the very low $\text{fT}/\sqrt{\text{Hz}}$ range. Assuming that the sensor noise is measured, it usually appears a frequency dependent noise at low frequency, the famous "1/f" excess noise. In order to quickly give an idea of their sensor noise, authors should give the white floor level, together with the knee frequency below which the excess noise is dominant. Note that noise studies are powerful tools for improving materials and sensor design, as well as to think up noise reduction techniques. SQUID people became expert in this art.

Giving the frequency dependent sensitivity, which is a way to make clear the system bandwidth, and the noise power spectrum enables the computation of useful parameters: namely the rms noise value, followed by the signal to noise ratio and the dynamic range. The former B_{rms} is deduced after integration over the bandwidth (full or user specified), and the second is the ratio of the signal (rms value) to B_{rms} . The last is the ratio, at a given frequency, of the largest signal to the lowest in a 1 Hz bandwidth. It is usually expressed in $\text{dB}/\sqrt{\text{Hz}}$. That quantity is useful when tracking very small signal occurring around large and slower variations. Typical example may be found in numerous applications of non-destructive evaluations, but also

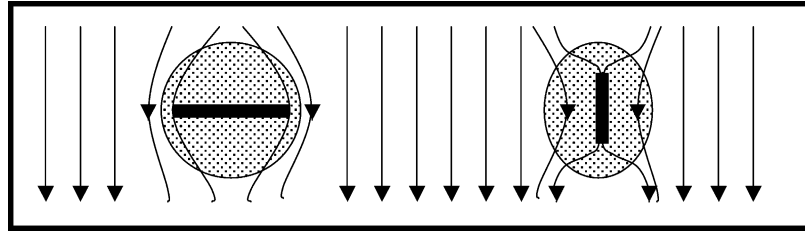


Fig. 1. Energy–volume criterion: schematic view of the field line bending by Meissner effect (left) or by high permeability material (right). The magnetic energy density, in the lack of the sensor, integrated on the drawn volume $\delta\Omega$, gives the energy resolution ε .

in noise reduction. Following the problematic of time varying large signals, the slew rate must be specified, as the maximum time rate at the output usually divided by the transfer function and expressed in T/s. Linearity of the sensor is also very important when designing a system for a specified application. It is conveniently expressed in terms of harmonic distortion. It must be noted here that the linearity of the bare sensor, is not a so relevant parameter. As a matter of fact, especially in the case of small sensors, it can be make a very efficient use of field feedback, with the known improvements of feedback systems compared to open loop systems.

Let me now discuss about energy resolution of magnetic field sensors, as a good tool to compare them, in relation with a volume based criterion. Many of magnetic sensors make good use of magnetic circuits or superconducting loops to input couple the incoming signals. By virtue of focusing effects, field lines are bent toward and through high permeability region, or excluded from superconducting materials due to Meissner effect, as roughly drawn on Fig. 1. The volume $\delta\Omega$ inside which the field lines are modified compared to the case without the sensor may then be used to get a rough estimate of the energy resolution ε :

$$\varepsilon \approx \frac{B_m^2}{2\mu_0} \delta\Omega, \quad (1)$$

where B_m is the mean field over $\delta\Omega$ (sensor off) and μ_0 the vacuum magnetic permeability. Even though that expression of energy resolution is only approximate, indeed it give the correct order of magnitude compared to more sophisticated theories describing each physics of the sensor, and it allows easy comparison of magnetic sensors, as is done for example with the noise energy of amplifiers. Examples will be given later.

Coming afterward is the spatial resolution. It is first related to the sensor's shape, for example planar for SQUIDs or thread for amorphous wires. It is often limited by the sensor encapsulation and wiring, or limited by cryogenic necessity. This give rise to a dead volume. Anyway, the problem of spatial discrimination between adjacent magnetic dipoles using magnetometers cannot be discussed without introducing the source—magnetometer separation. Nevertheless, a rough estimate of the optimum source—magnetometer distance can be the radius of the sphere whose volume is $\delta\Omega$.

Besides the previous specifications, it is also useful to consider the sensor ability to work in differential mode (gradiometry) and more sophisticated networks, the sensor ability for its

integration on semi conducting (superconducting) chips, and the sensor compatibility with digital signals which soon interfere after the preamplifier output stage.

3. A brief state of the art of SQUIDs sensors

SQUID literature became truly encyclopaedic, and it would be somewhat cumbersome to give a review upon it. As a matter of fact, SQUID's story began soon after the Josephson effects prediction and discovery in the early 1960s, but good, reproducible, Josephson junctions were available in the mid-1970s, making good use of niobium thin film and planar technologies. Nowadays, the technology is very well stabilized, with a few accessible foundries. SQUIDs are used in many laboratories, for many different applications. A large development of low T_c SQUID system was done for bio magnetism, especially for the magnetoencephalography. There are several SQUIDs species—radio frequency (rf), direct current (dc), relaxation SQUIDs (ROS), digital SQUIDs. The main features of these flux sensitive devices are related to their basic topology that is a small superconducting loop weakened by one or two Josephson junctions. The typical loop area lies in the $100 \mu\text{m} \times 100 \mu\text{m}$ range and the measured quantity is not the field itself, but rather its density, i.e. the magnetic flux basically passing through the superconducting loop. The flux noise spectral density lies in the range of 10^{-5} to $10^{-6} \Phi_0/\sqrt{\text{Hz}}$ where $\Phi_0 = 2.06 \times 10^{-15} \text{ Wb}$ is the flux quantum, and the associated field sensitivities $B_{n,\text{SQUID}}$ are just deduced from the flux noise divided by the loop's area then giving $0.2\text{--}2 \text{ pT}/\sqrt{\text{Hz}}$. The field sensitivity is further increased using superconducting flux transformers designed in various geometries, with a primary area much larger than the SQUID loop, and a secondary coil well matched to the SQUID loop. Large field density amplifications exceeding 100 then lead to the fT range, even lower. In the latter case, environmental noise cancellation becomes tremendously difficult. The energy resolution of the flux transformer—SQUID assembly can be roughly deduced from the above formulation, assuming that the active volume $\delta\Omega$ is that of a sphere lying on the primary circuit. Seeing that the typical area is 1 cm^2 , we obtain a sphere radius of 0.56 cm , and simplifying expression (1) we obtain:

$$\varepsilon_{\text{SQUID\&Transformer}} = 1.7 \times 10^6 B_n^2 r^3 = 10^{-30} \text{ J/Hz}, \quad (2)$$

for a low T_c SQUID at $1 \text{ fT}/\sqrt{\text{Hz}}$. Note that the energy resolution of the bare SQUID is better, expression (2) leading to 10^{-32} J/Hz with $B_n = 0.2 \text{ fT}/\sqrt{\text{Hz}}$ and $r = 50 \mu\text{m}$. This value is coherent with

Table 1
Relevant parameters of state of the art SQUIDs at PTB (Berlin), extracted from [8]

SQUID reference	Temperature (K)	Equivalent diameter (mm)	Field to flux transfer (nT/ Φ_0)	White noise (fT/ $\sqrt{\text{Hz}}$)	1/f knee frequency (Hz)	Bandwidth (MHz)	Slew rate ($\Phi_0/\mu\text{s}$)
W9L-18D9	4.2	7	0.46	0.9	2	2.3	0.4
W9SI-6E52	4.2	1.48	10.6	13	2	3.8	0.9
BY57	77	9	5.1	36	1.4	1.2	0.85

the standard SQUID theory, where:

$$\varepsilon_{\text{SQUID,Th}} = 16k_{\text{B}}TL/R = 9.3 \times 10^{-33} \text{ J/Hz}, \quad (3)$$

with k_{B} the Boltzmann constant, $T=4.2 \text{ K}$, $L=100\text{pH}$, and $R=10 \Omega$ (usual for the low T_{c} Josephson junctions). Indeed, these values have the correct orders of magnitude that are known to approach the fundamental value of the Plank's constant at very low temperature. At higher temperature, the energy resolution deteriorates, it can be estimated to $1.6 \times 10^{-26} \text{ J/Hz}$ for a high T_{c} SQUID such that presented in Table 1. Finally, to give a better view of the true SQUID state of the art, I just would like invite the reader to refer to papers of Drung at PTB, in Berlin [8,9]. To have a brief idea of what the state of the art is, some data are extracted from these papers, and gathered in Table 1. These data are obtained using advanced read out electronics, which are very compact, and include DSP (digital signal processor) based signal processing.

4. Recent developments in atomic vapor magnetometers

These magnetometers are generally referred as optically pumped magnetometers (OPM). Known since the early 1960s, a recent review of various magnetic effects in atoms may be found in [10]. During the 1970s, scalar magnetometers making good use of atomic vapor cell containing helium, cesium or potassium have been studied; some of them exhibited very low noise levels, down to the fT/ $\sqrt{\text{Hz}}$ level. No matter how, these will not be considered here, because of the too large volume of their cells (of the order of 1000 cm^3), and we want to restrict the review to those gas phase sensor having a volume comparable to the active volume of current solid phase sensor, i.e. of the order of 1 cm^3 . Nevertheless, those people interested may found commercial product together with technical descriptions in [11]. Recent researches have been carried out, which significantly reduced noise, leading to the small sensitive atomic vapor cells that are now considered. Two kinds of magnetometers can be considered, which are sensitive to the field magnitude or to field vector components. The first one has simple working principle, related to the coupling of suitable atomic species with the magnetic field via the atomic spin. The glass cell containing atoms may acquire a macroscopic magnetization M , the latter get in precession around the direction of the applied field B_{tot} , that occurs at the Larmor frequency ω_{L} given by:

$$\omega_{\text{L}} = \gamma|B_{\text{tot}}|, \quad (4)$$

where γ is the Lande factor of the atoms. For cesium atoms, $\gamma=21.99 \text{ rad/s/nT}$.

A measure, direct or indirect, of the Larmor frequency in polarized atomic vapor then lead to the field variations. The magnetization is generally obtained using circularly polarized laser beam, the transmitted power of which is detected. In the detecting scheme proposed in [12], a resonant mode is used together with a lock-in technique. It is experimentally demonstrated a noise level of 63 fT/ $\sqrt{\text{Hz}}$ (white noise), in a 140 Hz bandwidth, for a 20 mm long and 20 mm cell filled with 45 mbar Ne, 8 mbar Ar and a saturated Cs vapor. Since the laser beam is only 8 mm in diameter, and because the magnetized vapor has only a small effect on the mean field over the cell, the energy resolution (1) of that magnetometer can then be estimated to $1.6 \times 10^{-27} \text{ J/Hz}$. This nice result, was used to monitor clear MCG signals [13,14], using a gradiometric mode to reduce environmental noise. These signals are reproduced here in Fig. 2, to show the reality of room temperature magnetocardiography. Also plotted in Fig. 3 is a serie of real time MCG signals that were recorded a few years ago [15] using low noise flux gates, with a noise floor at 2–3 pT/ $\sqrt{\text{Hz}}$, 100 Hz bandwidth, moderate shielding or gradiometric mode. The magnetometers outputs are very similar, despite of a much better noise floor of the OPM. It can be thought that the later is still degraded by environmental noise, otherwise the signal to noise ratio should be about a factor 7 better using the OPM than using the low noise flux gate. However these results are very promising.

^4He is also used to produce some low noise, miniature magnetometer. Because it can also be used to sense very small fields around zero, it has been used together with three pairs of orthogonal coils in Helmholtz configuration. Currents through the three

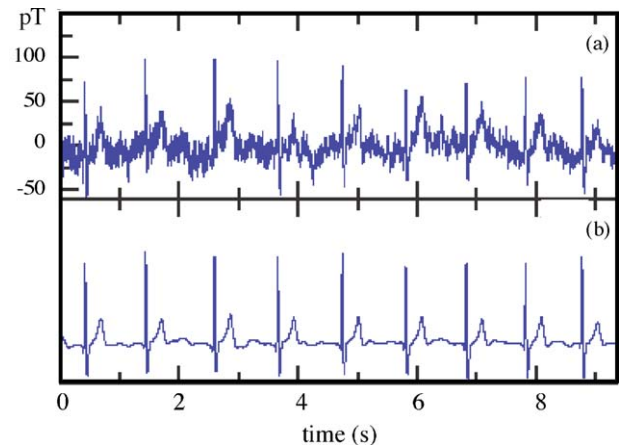


Fig. 2. MCG signals from the optical pumping magnetometer of the Fribourg's group [14, p. 904]. Curve (a) shows the gradiometer output, in a bandwidth of 140 Hz, and moderate shielding. Curve (b) is with signal processing.

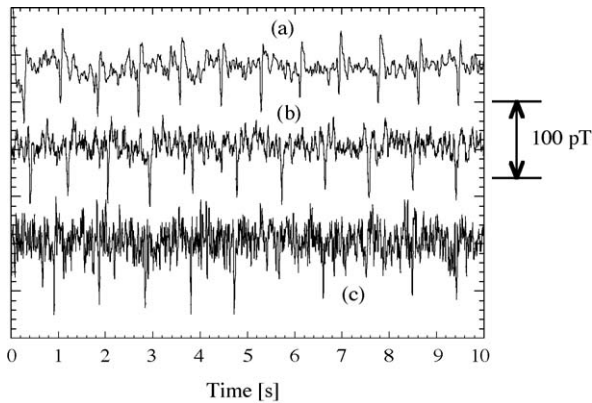


Fig. 3. MCG signals from a room temperature fluxgate from [15]. The curve (a) is inside a shielded room and 40 Hz bandwidth. Curve (b) is with moderate shielding, 100 Hz bandwidth and comb filter at 50, 100 Hz. Curve (c) is in a gradiometer configuration, without shields.

coils are feedback so that the total mean field in the cell remains always very close to zero. Reading the three currents then gives the three field components. That system is described in [16], where the field equivalent noise spectrum are reported, showing in both case noise floors about $2\text{--}5\text{ pT}/\sqrt{\text{Hz}}$ and a bandwidth in excess of 50 Hz. It should be pointed out that the process to get the three vector components make good use of a sampling technique, due to the necessary successive reading of the error field magnitude in each direction. This likely works as a kind of magnetic chopper, which after all gives a very significant reduction of $1/f$ noise in the $0.1\text{--}10\text{ Hz}$ band, compared to the scalar magnetometer. The energy resolution can also be deduced using (1) for the 6 cm^3 cell to give $\varepsilon = 10^{-23}\text{ J/Hz}$. To close the discussion on these two OPM, it appears that combining the two techniques [13,14,16] could lead to a vector magnetometer in the $100\text{ fT}/\sqrt{\text{Hz}}$ range, with improved low frequency noise.

Analysing the noise processes in atomic magnetometers, it is known that the mechanism of spin-exchange relaxation lead to a fundamental limit [17] where the collisions between two polarized atoms induce decoherence in the spins precession and signal loss. The Romalis group at Princeton has shown that this relaxation mechanism can be suppressed provided that the Larmor frequency is set down enough, and the atomic density high enough, leading to a characteristic relaxation time between collisions much higher than the Larmor period. This means that the total field B_0 in the vicinity of the cell must stay very small, together with a cell heating up to 180°C to get the required atom (potassium) density. A description of all the process and magnetometer may be found in [18]. The potassium cell is surrounded by a set μ -metal shields (shielding factor 10^6) to enough lower the earth field. The spin polarization is obtained using a high power laser diode, circularly polarized. A test field in one direction is applied using coils. The spins precession is detected using the beam emitted by a single frequency laser diode, linearly polarized. In virtue of the circular dichroism acquired by the vapor a rotation in the polarization angle of the beam crossing the cell is induced. The output signal is obtained using an array of photodiodes detecting the probe laser, after passing an analyzing polarizer. Spectrum of the noise equivalent field at the

magnetometer input were recorded, showing a level as low as $7\text{ fT}/\sqrt{\text{Hz}}$ above 20 and 140 Hz bandwidth, with an active volume of $4\text{ mm} \times 19\text{ mm} \times 40\text{ mm}$. That noise was limited by the Johnson noise of the conducting material (shields) surrounding the experiment. Using a gradiometer configuration allowed to reduce that noise down to $0.54\text{ fT}/\sqrt{\text{Hz}}$. Estimates of the energy resolution using (1) and the above data gives $\varepsilon = 7 \times 10^{-29}\text{ J/Hz}$ in the magnetometer configuration and $7 \times 10^{-31}\text{ J/Hz}$ in the gradiometer configuration. These results are truly impressive, because the cell is above room temperature, and because the theoretical fundamental noise floor is estimated to be $0.01\text{ fT}/\sqrt{\text{Hz}}$. The associated energy resolution of the latter would then be $1.2 \times 10^{-34}\text{ J/Hz}$, that of the best SQUIDs at the quantum limit. That opens competition between SQUIDs and the spin-exchange relaxation free (SERF) magnetometer, then start to be discussed. An undisputed opinion (for SQUID people) from Wikswow may be read in [19], which defends the SQUID technology for brain magnetic activity characterization.

5. Room temperature solid state magnetometers

The simplest device allowing the measurement of magnetic flux is done using coils and magnetic cores in linear regime to get small sizes. I will not detail these, because they do not work at dc, and the required size to get noise below the pT range is still to large in this review. The most popular magnetic sensor also makes good use of coils around saturable magnetic cores, feed with an ac pumping current. Known as flux gates, small size ones, a few centimeters long, reach the $\text{pT}/\sqrt{\text{Hz}}$ noise level. Although a tendency is towards their integration on silicon chips, I do not discuss them further, because the size reduction fundamentally leads to an intrinsic magnetic noise increase. Further, for the cubic centimeter scale ones, there were no large improvements these last years.

Since the end of the 1980s, where giant magneto-resistance effects have been discovered, progress have been regularly made, together with various devices such giant magneto-resistances (GMR), colossal magneto-resistance (CMR), spin valves, magnetic tunnel junctions. All these devices make good use of magnetic and conducting ultrathin layers, even insulating layers in the case of tunnel junctions. All these devices exhibit a strong dependency of their dc electrical resistance versus an applied magnetic field, with typical field coefficients $\frac{1}{R} \frac{dR}{dB}$ up to $70\%/Oe$. They mainly are designed for magnetic reading heads. Low field sensing is also addressed, but their intrinsic noise still is high. As a matter of fact, the search for a low Johnson noise implies the choice of low resistance values, say 50 or so ohms, together with the use of low voltage noise amplifiers, say $1\text{ nV}/\sqrt{\text{Hz}}$. On the other hand, the bias current of these devices cannot be arbitrarily high due to heating effects, and cannot exceed about 10 mA. It follows that the best devices reach the $\text{pT}/\sqrt{\text{Hz}}$ level and are just commercially available, but the excess low frequency noise commonly is much larger than that obtained in flux gates. A very interesting work was recently done [20,21], which make good use of a superconducting transformer coupled to a high quality GMR spin valve sensor, just as suggested in our previous review [1]. Fig. 4 depicts this hybrid magnetometer, which

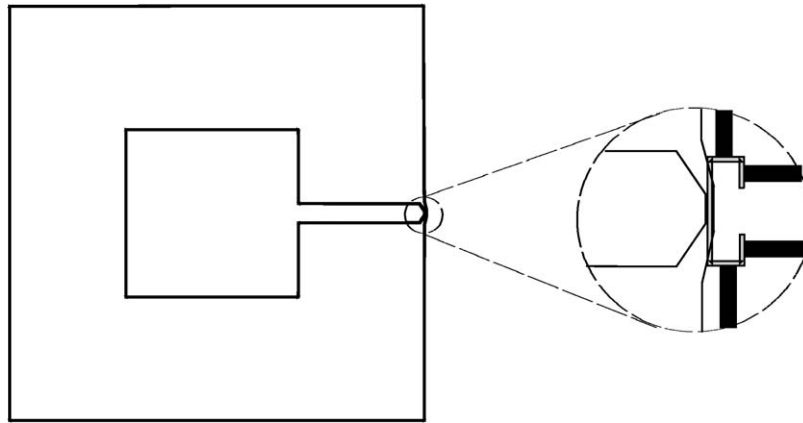


Fig. 4. Hybrid superconductor—GMR sensor redrawn after [20,21]. The large square is a superconducting washer, similar to a Ketchen square washer for SQUIDs. The gray pattern is that of the GMR in a yoke type shape $20\ \mu\text{m} \times 70\ \mu\text{m}$, and the black lines are for the contacts. The superconducting washer is about $1\ \text{cm} \times 1\ \text{cm}$.

exhibited field gains of 100 up to 80 K using a superconducting loop (6.5 mm diameter) coupled to the GMR. Noise floors were found at 30 and $100\ \text{fT}/\sqrt{\text{Hz}}$, with respective $1/f$ knee frequencies of 100 and 20 Hz at working temperature of 4.2 and 77 K, respectively. The associated energy resolutions also deduced from (2) are 5×10^{-29} and 5.5×10^{-28} J/Hz. These devices being very new, they appear extremely promising if the field gain can be increased by one or more order of magnitude, and/or if GMR with very large magneto-resistance can be used. In principle they could compete with SQUIDs.

Following that idea of an input circuit strongly coupled to a GMR, it is also interesting to consider what was recently done using a room temperature circuit [22] to obtain a large field feedback to the sensor, which in exchange improve the system linearity and enlarge the dynamic range. The encapsulated improved GMR with feedback is $0.7\ \text{mm} \times 0.7\ \text{mm} \times 4\ \text{mm}$, with a noise spectral density of $150\ \text{pT}/\sqrt{\text{Hz}}$ and a dynamic range close to $150\ \text{dB}/\sqrt{\text{Hz}}$ above 1 kHz, a very large slew rate measured at $0.37\ \text{T/ms}$. These performances are attractive in non-destructive evaluation using eddy current techniques [23]. Although the deduced energy resolution appears high (1.7×10^{-23} J/Hz), it must be pointed out that using such technique on lower noise floor devices, say at $1\ \text{pT}/\sqrt{\text{Hz}}$, should lead to resolution in the 10^{-27} J/Hz range with extremely large dynamic ranges.

Beside the magneto-resistive devices, the so-called magneto-impedance devices were introduced during the 1990s. An extensive review of the theory and applications with a complete set of references is found in [24]. Nevertheless, works on proper noise characterizations and models are just starting [25,26]. Compared to the GMR devices, they have much higher field sensitivity, with moderate dissipative part, which in principle could lead to low noise, expected at the sub-pT/ $\sqrt{\text{Hz}}$ level [1]. Measurements presented in [24] show a noise level of about $5\ \text{pT}/\sqrt{\text{Hz}}$ above 1 kHz, in an amorphous magnetic wire 4 mm long and about $35\ \mu\text{m}$ diameter. An estimate of the energy resolution then gives $5 \times 10^{-29}\ \text{J/Hz} < \epsilon < 3.2 \times 10^{-25}\ \text{J/Hz}$ according to the way the $\delta\Omega$ volume is estimated. Clearly, more works are needed to clarify the noise of this kind of sensor, always having in mind that the final system, sensor + bias + detection, should stay easy to use.

All the solid state magnetometers called to mind in this section, used magnetic and conducting materials, the latter subjected to the Johnson noise. It has been suggested that it could be interesting to use insulating, monodomain, magnetic material such yttrium iron garnet (YIG) excited by a rotating magnetic field [27], the amplitude of which being sufficiently large to saturate the sample. A theory has been developed [28] to show that the thermal noise of the magnetic material should be as low as $5.3\ \text{fT}/\sqrt{\text{Hz}}$ in a device 1 cm in diameter and $3.2\ \mu\text{m}$ in thickness. However, conducting coils needed to apply the rotating field and to pick up the output signal, strongly degrade the above fundamental limit, to about $0.4\ \text{pT}/\sqrt{\text{Hz}}$. Indeed, a few noise spectrums were presented which show this level was achieved [29]. The corresponding energy resolution is 3.2×10^{-27} J/Hz with the coil volume included and 1.6×10^{-29} J/Hz for the YIG crystal alone, whereas the fundamental limit should give about 3×10^{-33} J/Hz. It has also to be pointed out that the experimental results apparently showed a “ $1/f$ ” as low as 0.1 Hz. These works, both theoretical and experimental appear very attractive, and in my mind, the community working in magnetic sensing should much better take over them.

Finally, let us just mention the extraordinary magneto-resistance effect (EMR), first introduced in [30]. It occurs in hybrid micro- and nano-structures of non-magnetic materials and they are supposed to exhibit only the Johnson noise contribution, without the magnetic one [31]. The effect is shown at low temperature as well as at room temperature. The noise measurements reported in [31] are coherent with the Johnson noise as the dominant source in the device, the level of which was finally expressed in units of $\mu\Phi_0/\sqrt{\text{Hz}}$ to compare with SQUIDs. Due to the small area of the devices (less than $50\ \mu\text{m} \times 50\ \mu\text{m}$), we estimated the field resolution to be about $100\ \text{pT}/\sqrt{\text{Hz}}$ at 4.2 K, which is not so impressive, as claimed by the authors.

6. Conclusion

Writing this review on high sensitivity magnetometers, I tried to gather results published between years 2000 and 2004, in the spirit of what I have done for a previous review during year 2000. Anyway, it is very far to be exhaustive. By the year 2000, not

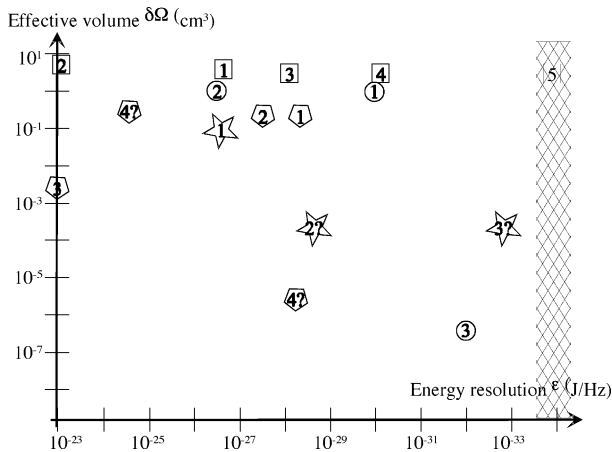


Fig. 5. Energy resolution–volume criterion. Circles are for SQUIDs (1: low T_c coupled, 2: high T_c , 3: low T_c bare). Squares are for OPM (1: Cs cell; 2: He cell; 3–5: K cell). Pentagons are GMR—GMI sensors (1, 2: hybrid GMR at 4.2 and 77 K; 3: GMR with feedback coil; 4?: GMI). Stars are for YIG magnetometer. The rectangular pattern at 10^{-34} is for the quantum limit. An ideal magnetometer should reach the quantum limit together with the smallest possible volume, but with realistic coupling to external signals.

much researchers dare to compare performances of their sensors to that of SQUIDs, above all the low T_c ones. Reading the references associated to this review shows this is no longer the case, even if often unjustified. I tried to clarify that situation, starting from comments on relevant sensors parameters which, in my mind, help engineers to select and buy sensors for given applications. I hope it will also help physicists searching new effects and new devices, to sometimes better give specifications of their devices. Among these parameters, I use a rough but convenient estimate of the magnetic energy resolution, based on an effective volume inside which the sensor operates and on the usual volumic density of magnetic energy. It appears to me it is convenient to quickly see whether or not a high sensitivity magnetic sensor compete or not with the best ones. Results are reported in Fig. 5. With this criterion, it is clear that only the SERF magnetometer is truly at the level of low T_c SQUIDs. The hybrid superconducting-GMR magnetometer is not very far, with technologies and size rather comparable to that of SQUIDs. In my opinion, competition could become very interesting between these two solid state, cryogenic devices. About the other solid state, room temperature, magnetic sensors reviewed here, it is still an issue to get a real system demonstrating a $100 \text{ fT}/\sqrt{\text{Hz}}$ noise level above 1 Hz, which would have a large set of interesting applications, unless the YIG magnetometer is more studied and affirmed by the magnetic sensor community.

References

[1] D. Robbes, C. Article Invité, S. Dolabdjian, Y. Saez, G. Monfort, P. Kaiser, Cioreanu, Highly sensitive uncooled magnetometers: state of the art superconducting magnetic hybrid magnetometers, an alternative to SQUIDs? PT ASC 2000, Virginia Beach, September 2000, IEEE Trans. Appl. Supercond. 11 (1) (2001) 629–634.
 [2] G. Bednorz, K.A. Müller, Possible high T_c superconductivity in the Ba–La–Cu–O system, Z. Phys. B 64 (1986) 189–193.

[3] J.M. Phillips, Substrate selection for high temperature superconducting thin films, J. Appl. Phys. 9 (4) (1996) 1829–1848.
 [4] P. Chaudary, J. Mannhart, D. Dimos, C.C. Tsuei, J. Chi, M.M. Opreysko, M. Scheurmann, Phys. Rev. Lett. 60 (1988) 1653.
 [5] H. Koch, SQUID magnetocardiography: status and perspectives, IEEE Trans. Appl. Supercond. 11 (1) (2001) 49–59.
 [6] I. Tavarozzi, S. Comani, C. Del Gratta, S. Di Luzio, G.L. Romaniş, S. Gallina, M. Zimarino, D. Brisinda, R. Fenici, R. De Caterina, Ital Heart J. 3 (3) (2002) 151–165.
 [7] S.H. Liao, S.C. Hsu, C.C. Lin, H.E. Horng, J.C. Chen, C.H. Wu, H.C. Yang, High- T_c SQUID gradiometer system for magnetocardiography in an unshielded environment, Supercond. Sci. Technol. 16 (2003) 1426–1429.
 [8] D. Drung, High- T_c and low- T_c dc SQUID electronics, Supercond. Sci. Technol. 16 (2003) 1320–1336, Online at stacks.iop.org/SUST/16/1320.
 [9] D. Drung, High-performance DC SQUID read-out electronics, Physica C 368 (2002) 134–140.
 [10] D. Budker, W. Gawlik, D.F. Kimball, S.M. Rochester, V.V. Yashchuk, A. Weis, Resonant nonlinear magneto-optical effects in atoms, Rev. Mod. Phys. 74 (4) (2002) 1153–2002.
 [11] <http://www.gemsys.ca/current/index.html>.
 [12] G. Bison, R. Wynands, A. Weis, Optimization and performance of an optical cardio-magnetometer, arXiv:physics/0406157 v1 30 Jun 2004.
 [13] G. Bison, R. Wynands, A. Weis, A laser-pumped magnetometer for the mapping of human cardio-magnetic fields, Appl. Phys. B 76 (2003) 325–328.
 [14] G. Bison, R. Wynands, A. Weis, Dynamical mapping of the human cardiomagnetic field using a room temperature, laser-optical sensor, Opt. Express 11 (8) (2003) 904–909.
 [15] C. Dolabdjian, S. Saez, A. Reyes Toledo, D. Robbes, Signal to noise improvement of biomagnetic signals using a flux gate probe and a real time signal processing, Rev. Sci. Instrum. 69 (10) (1998) 3678–3680.
 [16] R.E. Slocum, L. Ryan, Earth Science Technology Conference on Self-calibrating Vector Magnetometer for Space, Pasadena Hilton, Pasadena, CA, 11 and 13 June, 2002, paper B3P4. web address: [esto.nasa.gov/conferences/estc-2002/Papers/B3P4\(Slocum\).pdf](http://esto.nasa.gov/conferences/estc-2002/Papers/B3P4(Slocum).pdf).
 [17] D. Buckler, D.F. Kimball, S.M. Rochester, V.V. Yashchuk, M. Zolotarev, Sensitive magnetometry based on non-linear magneto-optical rotation, Phys. Rev. A 62 (2000) 043403.
 [18] I.K. Kominis, T.W. Kornack, J.C. Allred, M.V. Romalis, A subfemtotesla multichannel atomic magnetometer, Nature 42 (2003) 596–599.
 [19] J.P. Wikswo, SQUIDs remain best tool for measuring Brains’s magnetic field, Phys. Today February (2003).
 [20] M. Pannetier, C. Fermon, G. Le Goff, J. Simola, E. Kerr, Femtotesla magnetic field measurement with magnetoresistive sensors, Science June (2004).
 [21] M. Pannetier, C. Fermon, G. Legoff, E. Kerr, Ultra-sensitive mixed sensors—design and performance, paper M-P.30, this conference.
 [22] L. Perez, C. Dolabdjian, W. Waché, L. Butin, Advance in magnetoresistance magnetometer performances applied in eddy current sensors arrays, in: Proceedings of the 16th World Conference on Non-destruction Testing, Montreal, Canada, August 30–September 3, 2004.
 [23] L. Perez, J. Le Hir, C. Dolabdjian, L. Butin, Investigation of fatigue cracks under rivet head airframe using improved GMR magnetometer in an eddy current system, J. Electrical Eng. 55 (10/S) (2004) 10–11.
 [24] M. Knobel, M. Vazquez, L. Kraus, in: J. Buschow (Ed.), Handbook of Magnetic Materials, vol. 15, Elsevier, 2003, pp. 497–563 (Chapter 5).
 [25] D. Ménard, G. Rudkowska, L. Clime, P. Ciureanu, A. Yelon, S. Saez, C. Dolabdjian, D. Robbes, Progress towards the optimization of the signal-to-noise ratio in giant magnetoimpedance sensors, this conference.
 [26] A. Boukhenoufa, C. Dolabdjian, D. Robbes, High sensitivity giant magneto-inductive magnetometer characterization implemented with a low frequency magnetic noise reduction technic, Rev. Scientific Instrum., in press.
 [27] P.M. Vetoshko, V.B. Volkovoy, V.N. Zalagin, A.Yu. Toporov, J. Appl. Phys. 70 (1991) 6298–6300.

- [28] P.M. Vetoshko, M.V. Valeiko, P.I. Nikitin, Epitaxial yttrium iron garnet film as an active medium of an even-harmonic magnetic field transducer, *Sens. Actuators A* 106 (2003) 270–273.
- [29] M.V. Valeiko, P.M. Vetoshko, P.I. Nikitin, Proceedings of the Third EMSA Conference, Dresden, July 19–21, 2000, pp. 141–142.
- [30] S.A. Solin, T. Thio, R.R. Hines, J.J. Heremans, *Science* 289 (2000) 530.
- [31] C.H. Müller, O. Kronenwerth, Ch. Heyn, D. Grundler, Low noise magnetic flux sensors based on the extraordinary magnetoresistance effect, *Appl. Phys. Lett.* 84 (17) (2004) 3343–3345.